

Study on fuel/air mixing based on oblique detonation engine

Gaoxiang Xiang (✉ xianggx@nwpu.edu.cn)

Northwestern Polytechnical University

Danyang Li

Northwestern Polytechnical University

Xu Zhen Xie

Northwestern Polytechnical University

Qirong Tu

Northwestern Polytechnical University

Yi Chen Zhang

Northwestern Polytechnical University

Ke Jin

Xidian University School of Aerospace Science and Technology

Research

Keywords: Hypersonic, Oblique detonation, Fuel mixing, Numerical simulation,

Posted Date: July 6th, 2022

DOI: <https://doi.org/10.21203/rs.3.rs-1751780/v1>

License:  This work is licensed under a Creative Commons Attribution 4.0 International License.

[Read Full License](#)

Abstract

Currently, the inflow conditions used in the study of oblique detonation engines are ideal premixed inflow, and there are few studies on non-premixed inflow. The fuel mixing process in the flow field structure and mixing degree for forming oblique blast waves has essential significance. This paper uses a combination of theoretical analysis and numerical simulation to study the inlet section of the oblique detonation engine. The governing equations are the inviscid Euler equations coupled with chemical reaction source terms, and the second-order TVD scheme is used to solve the equations. First, this paper compared the influence of the single hydrogen nozzle parameters on the flow field structure and the hydrogen mole fraction distribution at the outlet, optimized the hydrogen jet structure, and analyzed the coupling effect between the incoming flow and the jet. The closer the nozzle location is to the supersonic inlet, the lower the Mach number, and the higher the equivalence ratio of hydrogen to oxygen, the better the fuel and air mixing effect. And too large or too small hydrogen injection angle will make the hydrogen too concentrated on the wall and insufficient penetration depth, which reduces the mixing of hydrogen. Secondly, while maintaining the same fuel mass flow rate as the single hydrogen nozzle, this paper increases the number of hydrogen nozzles, thereby increasing the obstruction to the incoming flow and improving the fuel mixing effect. Finally, because the physical ramp and aerodynamic ramp as a method of increasing mixing will lead to fuel concentration on the wall, which is not conducive to the subsequent combustion, this paper proposes an optimization model of the strut injection method. The results show that strut injection can effectively improve the mixing degree of hydrogen and air at the exit and solve the problem of fuel concentration at the wall by using the staggered jet and baroclinic effect of hydrogen. This paper reveals the law of fuel injection in the inlet and provides essential data support for studying oblique detonation engines in a non-premixed environment.

1. Introduction

The scramjet has the disadvantages of low combustion efficiency and short combustion time, and it is difficult to burn sufficiently and achieve adequate or higher propulsion efficiency. Therefore, the combustion mode of higher efficiency for the propulsion system-detonation engine is proposed^[1-4]. The detonation engines include pulse detonation engines, rotational detonation engines, and oblique detonation engines (ODE)^[5-7]. The oblique detonation wave is generated by self-ignition caused by the fuel compression by a leading shock wave. The fuel is injected at the front end of an air inlet of the aircraft, the detonation of the oblique detonation wave is induced by a shock wave generated by a wedge surface at the lower end of a combustion chamber, and the energy is rapidly released and accelerated through the expansion of a tail nozzle to generate strong thrust (Fig. 1 shows)^[8, 9]. The ODE has attracted extensive research; its post-wave chemical reaction is more intense and full, with a better diffusion combustion rate and high propulsion potential of nearly isovolumetric combustion^[10, 11]. The detonation of an oblique detonation wave involves strongly coupled nonlinear problems with multiple parameters such as excitation and combustion, and the conditions required for experimental studies are extremely high. It is difficult to control the combustion process effectively. Therefore, numerical simulations to study

the detonation mechanism of oblique engines are becoming a cost-effective method. In most previous studies, work has been carried out on the wave system structure of the detonation, the detonation mechanism, and the stability of the detonation wave^[5, 8, 10, 12, 13]. Most of the current research uses the gas flow prerequisites are ideal premixed incoming flow, so the non-premixed incoming fuel mixture for the study of the formation mechanism of the oblique detonation wave and the flow field structure is of great importance.

The fuel residence time is in the millisecond range for supersonic or hypersonic incoming flows. The incompressible shear layer created by the flow field results in a much slower mixing rate between the fluids than incompressible fluids. Suppose the atomization and evaporation processes of liquid hydrogen fuel and the conditions of the inlet tract and combustion chamber are taken into account. In that case, it is even more difficult to achieve the ideal fuel mixture with the incoming flow. Active and passive mixing enhancement techniques have been proposed by domestic and foreign scholars and summarized in a review by domestic scholars^[14]. The physical ramp is an effective device to enhance blending. Abdel-salam^[15] et al. found that increasing the slope back-swept angle can increase the mixing efficiency while increasing the incoming Mach number will lead to a decrease in mixing efficiency. However, because the physical ramp surface must be ultra-high heat resistant and geometry dependent, it is gradually replaced by pneumatic ramps in more demanding theoretical studies. Pneumatic ramps are mainly used to enhance the blending efficiency by arranging the array of fuel holes on the wall and using the obstruction effect of multiple holes on the incoming flow. Commonly, there are four-hole and nine-hole pneumatic ramp configurations. Fuller^[16, 17] studied the structural properties of a nine-hole pneumatic ramp in a Mach number 2 flow field and found that the mixing efficiency of a pneumatic ramp in the near field is better than that of the physical ramp when the dynamic pressure ratio is the same. If the dynamic pressure ratio of the pneumatic ramp nozzle is increased, the mixing effect in the far-field can be similar to that of the physical ramp. In addition to the above mixing enhancement techniques based on flow vortex, concave cavity mixing enhancement^[18] techniques, mixing enhancement techniques with lateral curvature, and active mixing enhancement. Despite the advantages and disadvantages of various complex doping techniques, in most current research, physical ramp and aerodynamic ramp enhancement are still the most respected techniques. The simple configuration and uniform grid distribution of the slope reinforcement structure are beneficial to the numerical simulation study in this paper.

The current domestic and foreign scholars for oblique detonation research mainly focus on premixed incoming flow environment, and non-premixed environment is less studied. Fusina G^[19] studies the non-ideal incoming flow of non-stationary problems and analyzes the impact characteristics of wavefront perturbation of oblique detonation waves. While for the non-homogeneity of fuel mixing^[20, 21], Sicilian J P^[22] studied the structure of oblique detonation waves in two configurations of oblique detonation engines with non-uniform premixing.^[23, 24] Fang Yishen studied the variation of the initiation zone of oblique detonation wave and its influence on the position of the downstream wave surface in view of the non-uniformity of equivalence ratio of the incoming flow and found that the wall equivalence ratio mainly

affects the length of induction zone and the variation of equivalence ratio of main flow field mainly affects the position of wave surface^[25]. Studying oblique detonation engines under non-premixed incoming flow conditions is of excellent value.

In this paper, hydrogen is used as a fuel, which has a simple chemical formula for combustion compared to methane and acetylene and has a very low content in the air, which facilitates the differentiation of air and the observation and analysis of the basic structure of the flow field. Secondly, the density of hydrogen gas is very low, and the speed of sound is very high. With equal mass flow rate and Mach number, the jet's momentum is higher, the penetration depth is greater, and the intensity of the resulting surge is stronger. In this paper, through the establishment of the forward port model of the oblique detonation wave engine, considering the inflow conditions at a relatively real altitude of 30 km/H,

according to the equivalence ratio of hydrogen and oxygen, the position of the fuel nozzle, the injection angle and the Mach number of incoming flow, the complex flow field structure, and the mixing effect of fuel are discussed and studied.

2. Physical Model And Numerical Methods

This paper addresses the oblique detonation engine intake as the object of study (Fig. 1); the study selected air incoming Mach numbers of 5, 7, and 9, respectively. The calculation area as shown in Fig. 2, the red dotted line within the region, the coordinates of the calculation domain to match the schematic, the direction of air incoming flow for the positive direction of the x-axis, and the y-axis is perpendicular to the direction of air incoming flow up.

This paper addresses the fuel mixing characteristics of a slant-detonation engine intake in a restricted space and the structural complexity in engineering applications. The model is simplified, retaining the main structure of the intake tract, and constructed in two dimensions.

In order to ensure the grid quality and orthogonality, the blank area in the lower part of the wall in the red dashed box in Fig. 1 is used as the computational domain, as shown in Fig. 2. The physical model is 620 mm in total length, 450 mm in x-direction projection of the first wedge, and 150 mm in x-direction projection of the second wedge, and a 20 mm long computational domain is set at the front of the inlet to reflect the more realistic hypersonic incoming flow, considering the escape of the incoming air into the inlet. The angle between the first wedge surface and the x-positive direction θ_1 is 15° , and the angle between the second wedge surface and the x-positive direction θ_2 is 30° . In the study of the mixing of hydrogen and air with different parameters, the control variable method is used to change one of the parameters of hydrogen-to-oxygen equivalent ratio, incoming Mach number, hydrogen nozzle position, and hydrogen injection angle, and keep the other parameters constant.

When studying the degree of fuel blending, it is necessary to consider the basic parameters of the operating environment (30 km altitude): the atmospheric temperature is $T_0 = 226.51$ K, and the

atmospheric pressure $p_0 = 1197.0$ Pa. The sound velocity of the air in this operating environment can be calculated according to the following Eq. 1:

$$\alpha_{air} = \sqrt{r \cdot Rg_{air} \cdot T_0}$$

1

Where r is the specific heat ratio of diatomic molecules, i.e., 1.4; $Rg_{Air} = R/M$ is the gas constant of air, $R = 8.314$ J/(mol-K) is the ideal gas constant, and $M = 0.02896$ kg/mol is the molar mass of air. The specific parameters are shown in Table 1.

Table 1
Atmospheric parameters at 30 km

H[km]	T_0 [K]	P_0 [Pa]	ρ_0 [kg/m ³]	α [m/s]
30	226.51	1197.0	1.84E-2	301.68

Depending on the incoming Mach number and the angle of hydrogen injection, the static pressure at the hydrogen nozzle and the static temperature will also vary, and the static pressure at the hydrogen nozzle will be different when using single, double, and triple hydrogen nozzles, which is calculated using the controlled flow method, i.e., the air flow mass \dot{m}_{air} in the inlet tract is controlled by the Mach number of the incoming airflow M_{air} for a given inlet tract cross-section L_{air} , the required flow rate at the hydrogen nozzle is given by the number of moles of hydrogen required for the hydrogen-oxygen reaction and combined with the equivalence ratio $ER\dot{m}_{H_2}$, and thus the total fuel pressure required in the sonic throat is calculated as

$$\dot{m}_{air} = \rho \cdot \alpha_{air} \cdot M_{air} \cdot L_{air}$$

2

$$\dot{m}_{max} = \sqrt{\frac{r}{R}} \left(\frac{2}{r+1} \right)^{\frac{r+1}{2(r-1)}} \frac{p_0}{\sqrt{T_0}} A^* = 0.01062 \frac{p_0}{\sqrt{T_0}} A^*$$

3

Where \dot{m}_{max} is the maximum hydrogen fuel flow rate of the sonic throat, r and R are the adiabatic index and gas constant of the fuel, respectively, p_0 and T_0 are the total pressure and total temperature of the fuel, respectively, and A^* is the normal area of the acoustic throat, i.e., the hydrogen nozzle, and since the model is a two-dimensional model, the A^* is replaced by L_{H_2} . By changing the definition of the incoming Mach number and the hydrogen injection angle, the static pressure of the hydrogen nozzle can be obtained for different incoming Mach numbers and injection angles. The conversion equations of static pressure to total pressure and static temperature to total temperature are shown in Eqs. 4 and 5.

$$\frac{P}{P_0} = \left(1 + \frac{r-1}{2} M_a^2\right)^{-\frac{r}{r-1}}$$

4

$$\frac{T}{T_0} = \left(1 + \frac{r-1}{2} M_a^2\right)^{-1}$$

5

The hydrostatic pressure at the hydrogen nozzle for an equivalent ratio of 1.2 is calculated as shown in Table 2, and the angle of injection is the angle with the positive direction of the x-axis.

Table 2
Static pressure at the hydrogen orifice at an equivalent ratio of 1.2

Spraying Structure	incoming flow Mach number [Ma]	Spraying Angle	Static pressure [Pa]
Single spray	5	90°	89367.9
		45°,165°	241699
		90°	125115
Double spray	7	90°	160862
		35°,175°	176670
		55°,155°	94004.5
Triple spray	7	90°	62557.5
		30°,180°	155642
		45°,165°	80566.3
		60°,150°	56969.3
		90°	41705

The calculated hydrostatic pressure at the hydrogen orifice for an equivalent ratio of 4 is shown in Table 3.

Table 3
Static pressure at the hydrogen orifice at an equivalent ratio of 4

Spraying Structure	incoming flow Mach number [Ma]	Spraying Angle	Static pressure [Pa]
Single spray	5	90°	297659
	7	45°,165°	569254
		90°	416723
Double spray	7	90°	535787
		35°,175°	350889.5
		55°,155°	245695.5
Triple spray	7	90°	208461.5
		30°,180°	268349
		45°,165°	189751.33
		60°,150°	154931.33
		90°	138907.67

In this paper, we study the mixing of hydrogen in the supersonic incoming flow in the two-dimensional viscosity-free case, and we need to verify whether the mixing process occurs with combustion, so the controlling equation of the flow is the Euler equation with coupled chemical reaction source terms. The equations are in the form of Eqs. 2–7 as follows.

$$\frac{\partial U}{\partial t} + \frac{\partial F}{\partial x} + \frac{\partial G}{\partial y} = S$$

6

Among them.

$$U = \begin{bmatrix} \rho_1 \\ \vdots \\ \rho_n \\ \rho u \\ \rho v \\ E \end{bmatrix}, \quad F = \begin{bmatrix} \rho_1 u \\ \vdots \\ \rho_n u \\ \rho u^2 + p \\ \rho uv \\ (E + p)u \end{bmatrix},$$

$$G = \begin{bmatrix} \rho_1 v \\ \vdots \\ \rho_n v \\ \rho v u \\ \rho v^2 + p \\ (E + p)v \end{bmatrix}, \quad S = \begin{bmatrix} \omega_1 \\ \vdots \\ \omega_n \\ 0 \\ 0 \\ 0 \end{bmatrix}.$$

7

The subscript i represents the components in the primitive reaction, and n is the number of components; ρ is the mixture density, which can be expressed as the sum of the component densities ρ_i . u and v are the airflow velocities in the x and y directions, respectively, and p is the pressure. E is the total energy per unit volume, which can be expressed as

$$E = \rho h - p + \frac{1}{2} \rho (u^2 + v^2)$$

8

where h is the specific enthalpy. Where R_u is the universal gas constant, and W_i is the molar mass of component i . ω_i is the mass production rate per unit volume of the i -th component.

For the engine to work properly, in addition to considering whether there will be premature detonation in the combustion chamber, it is equally necessary to investigate whether in the intake tract, where the incoming air and hydrogen jets have been compressed by two wedge surfaces, the rise in the post-wave temperature of the oblique excitation wave formed by the mutual coupling of the two and the bow-shaped excitation wave formed by the two will cause premature fuel combustion to occur. The 9-component 19-reaction of the Jachimowsk reaction model^[26] was used in testing the presence of premature combustion in the intake tract. The product of combustion of hydrogen with oxygen in water, so it is possible to observe, based on the molar fraction distribution of each component in the calculated results, whether there is premature combustion. The results are shown in Fig. 3. In the whole flow field, components OH and H₂O are not present, which can indicate that this model does not occur in the intake tract of the possibility of premature combustion.

In this paper, the above equations are solved by a second-order TVD-type finite volume method, where the HLLC (Harten-Lax-van Leer Contact) approximate Riemann solver for the interface fluxes is used for calculation. The time advance is performed by the fourth-order Runge-Kutta method, and the CFL number controls the time step.

In order to verify the grid independence, three grids with different coarse and fine mesh numbers of 570000, 2280000, and 4560000 are used under the same initial conditions. From their pressure and temperature clouds, the results obtained from numerical simulations using grids with two grid resolutions of different coarseness and fineness are the same, so the small grid model is sufficient for calculation.

3. Results And Discussions

3.1 Flow field structure and mixing characteristics

When modeled as a single nozzle injected hydrogen structure, as shown in Fig. 4, the incoming flow is compressed by the wedge surface when it passes through the first wedge surface, forming an oblique shock wave (OSW) with an increased pressure after the wave, after the jet hydrogen injected from the sonic throat enters the engine intake tract, After the hydrogen is injected into the jet through the sonic throat at the speed of sound, the local pressure of the hydrogen jet continuously decreases, which is caused by the rapid expansion of the under-expanded sonic jet. The jet is compressed by the supersonic incoming flow after ejection and is reflected in the positive direction of the x-axis. While the supersonic incoming flow is flowing at high speed along the x-axis, it is blocked by the hydrogen jet ejected from the sonic throat, forming a Jet Shock Wave (JSW). Since the Mach number of the air incoming flow is much larger than the Mach number of the hydrogen jet, the surge receives a deflection as it progresses downstream, forming a bow-shaped surge at the windward end of the jet. The contour of Mach number 1 is marked in the figure, and the area surrounded by the contour is the subsonic region with a Mach number less than 1. Between the subsonic and supersonic regions, a supersonic jet is formed. In the supersonic jet region after the oblique excitation wave, another transmission excitation wave is formed, like the type IV excitation wave interference structure. While the generation of bowed excitation wave leads to the pressure rise after the excitation wave, the hydrogen expands after the jet, and the compression wave generated at the second wedge surface makes the mixed incoming flow of hydrogen and air expand again, which is favorable to the mixing of hydrogen and air.

When modeled as a dual-jet hydrogen injection, as shown in Fig. 5, at the front of the inlet tract, the structure is the same as that produced by a single hydrogen jet. Unlike the single hydrogen nozzle, a second jet surge is generated as the mixed fluid meets and couples with the hydrogen jet again when passing through the second hydrogen nozzle. The pressure and temperature after the wave increase again. The second surge has a negligible effect on the mixed fluid after the first, and the surging intensity is slightly less than the first. Subsequently, the same as the single jet. And a low-temperature zone was formed near the wall, which is because all the hydrogen is concentrated at the wall, and the hydrogen is formed at a lower temperature.

When the grid is modeled as a triple orifice for hydrogen injection, as shown in Fig. 6, the flow field structure is the same as that of the double orifice.

3.2 Effect of hydrogen nozzle parameters on mixing characteristics

The position of the fixed hydrogen nozzle is located at the first wedge plane, 100 mm from the y-axis, and the Mach number of the incoming air is 7. The angle of hydrogen injection is along the y-axis downward and perpendicular to the incoming flow direction, which is a transverse jet. The hydrogen to oxygen equivalent ratio is set to $ER = 1.2$ and $ER = 4$, respectively.

As the hydrogen-oxygen equivalent ratio increases, the intensity of the resulting oblique excitation increases. When the Mach number of the incoming airflow is fixed, the angle of hydrogen injection is fixed, and the rest temperature of hydrogen does not change, the hydrogen-oxygen equivalent ratio is proportional to the resting pressure at the hydrogen nozzle.

The increase in the equivalent ratio caused an increase in the static and total pressure at the acoustic throat, which enlarged the contact area between hydrogen and oxygen. It slightly increased the penetration depth of hydrogen, enhancing the mixing efficiency.

From the hydrogen mole fraction distribution curves of different equivalence ratios at the outlet (Fig. 8), it can be proved that increasing the hydrogen-oxygen equivalence ratio is beneficial to increasing the mixing efficiency of hydrogen with the incoming flow and has a higher fuel penetration depth (Fig. 7). Therefore, this paper will not consider the effect of the hydrogen-oxygen mixing equivalent ratio on the combustion zone in order to facilitate the search for different fuel injection structures in the front intake tract of the oblique detonation engine flow field distribution pattern and the effect of the degree of hydrogen mixing, the calculation after this section, the hydrogen-oxygen equivalent ratio is set to 4.

The hydrogen to oxygen equivalent ratio is set to 4, the Mach number of the fixed air incoming flow is 7 Ma, and the hydrogen injection angle is a transverse jet along the -y axis perpendicular to the air incoming flow. Three separate hydrogen vents are set in this section. The hydrogen vents are located on the first wedge surface, where the first hydrogen vent is 100 mm from the y-axis, the second hydrogen vent is 200 mm from the y-axis, and the third hydrogen vent is 300 mm from the y-axis. During the operation of one of the vents, the other vents are set as non-stick wall surfaces.

The results are shown in Fig. 9. When the distance between the hydrogen nozzle and the supersonic inlet increases, the hydrogen is mixing degree at the outlet decreases. This is because the closer the inlet, the more hydrogen, and air can fully use the length of the inlet to complete the mixing.

The hydrogen to oxygen equivalent ratio ER is still 4. The hydrogen nozzle's position is at 100 mm from the y-axis, and the hydrogen injection angle is a transverse jet along the -y-axis perpendicular to the incoming flow. The incoming Mach numbers are set to 5, 7, and 9, respectively.

As can be seen from Fig. 10, at smaller incoming Mach numbers, the hydrogen jet is more likely to reach large penetration depths, thus affecting the molar fraction distribution of hydrogen at the outlet, as

evidenced by Figs. 3–9, at increasing incoming Mach numbers, the molar fraction distribution of hydrogen at the outlet is significantly reduced.

The hydrogen-to-oxygen equivalent ratio and nozzle position are the same as in the previous section, the incoming Mach number is set to 7 in this section, and the hydrogen injection angles are 45°, 90°, and 165° (clockwise from the positive direction of the x-axis).

The molar fraction distribution cloud of hydrogen in Fig. 11 illustrates that the fuel injection angle also affects the deflection of the hydrogen jet. A small injection angle brings the hydrogen fluid closer to the wall. The decrease in injection angle also reduces the penetration depth. Therefore, a decrease in the fuel injection angle directly leads to a decrease in the mixing of air and hydrogen. The large injection angle also leads to the insufficient penetration depth of hydrogen, which makes the mixing of hydrogen less efficient. This is also clarified by the molar distribution curve of hydrogen at the outlet in Fig. 11(d).

In this section, the mixed flow fields of single, double, and triple hydrogen nozzles are numerically simulated with hydrogen jets located at 100 mm, 200 mm, and 300 mm from the y-axis, respectively. The hydrogen-oxygen equivalent ratio is 4, and the incoming Mach number is 7. The hydrogen is injected along the -y axis perpendicular to the incoming flow, and the mass flow rate of the controlled multi-hydrogen nozzle is the same as that of the single-hydrogen nozzle, as shown in Fig. 12. The comparison shows that the hydrogen distribution at the outlet of the triple hydrogen is significantly better than the latter two when it has the same total hydrogen injection flow rate as the single hydrogen orifice and the double hydrogen orifice.

3.3 The fuel/air mixing characteristics of strut injection method

The hydrogen distribution at the exit of the wall injection shows that the mixing effect is not ideal, especially for a high Mach number where the mixing effect is still limited. Both multi-jet and single-jet hydrogen injections show a concentration of hydrogen at the wall due to its insufficient penetration depth, which makes it difficult to mix uniformly and ideally with the incoming airflow within a brief time and short distance. In addition to wall injection, fuel injection in the mainstream can make the mixing not limited by the penetration depth and thus achieve a better mixing effect. Sislian^[26] et al. have conducted more research on the injection of hanging rod arms, while the direct-connected experimental system of the oblique detonation engine at the National Defense University of Science and Technology uses an array of nozzles for fuel mixing^[16]. Zhang Zijian^[17] Numerical calculations also show that with the direct injection of fuel in the mainstream through the strut transverse injector, after a period of time, the flow field is more uniformly distributed in the spreading direction, and the mixing effect is better, to facilitate the subsequent design of the oblique detonation engine.

This chapter adds the strut for injection mixing based on the intake tract configuration in the previous chapter. Zhang Zijian performed numerical calculations for simultaneous injection mixing of three

struts^[27], but the literature^[26, 27]. However, the experiments conducted in the literature only used single- or double-strut injection mixing, and no relevant numerical calculations appeared. Therefore, in this section, numerical simulations of the single-strut and two-strut injection mixing are performed to compare the differences between the two, as shown in the following figure.

According to Fig. 13, the hydrogen nozzle forms a stronger jet surge in front of it due to fuel injection in both the upper and lower strut injection, and the surge formed by the strut is weaker and has less influence on the jet surge. The stronger jet surge formed at the wall surface had a greater effect on the flow field, and the shape of the surge formed at the compression surface became curved. The flow direction also changed after the hydrogen jet passed through the surge. Because of the higher density after the surge, the hydrogen jet becomes thinner visually from the hydrogen mass fraction cloud diagram, as shown in Fig. 14. The cloud diagram of the molar fraction distribution of hydrogen also shows that the hydrogen injected from the upper strut at the exit is more uniformly mixed, and the diagram shows a lime green color between the blue air and the red color of hydrogen. In contrast, the hydrogen at the exit of the lower strut appears to be more concentrated. This is because the fuel layer of hydrogen injected from the upper strut is the first to interact with the main oblique excitation wave. The oblique pressure effect produced by the oblique excitation wave and the density gradient has the effect of enhancing the mixing. Secondly, the higher density within the main excitation layer can accelerate the diffusion efficiency of hydrogen in the air, which also belongs to the enhanced mixing.

In the case of simultaneous injection of two-struts, the flow field is not only the primary oblique surge formed by the compression of the two wedge surfaces in the inlet tract but also the secondary oblique surge formed by the obstruction of the incoming flow by the struts and the jet surge formed by the injection of hydrogen into the incoming airflow. The influence of the secondary oblique excitation on the flow field is weak compared with the other excitation waves, so it is difficult to be shown in the figure. It can be seen from Fig. 15 that the hydrogen mixing effect of the double-strut injection is significantly better than that of the separate injection of the upper and lower struts. This is because when the upper and lower struts are injected simultaneously, the hydrogen gas stream is staggered, i.e., the hydrogen jet on the lower side of the upper strut is staggered with the hydrogen jet on the upper side of the lower strut, which helps the mixing of hydrogen gas and air. Secondly, the high-pressure hydrogen gas is sprayed into the low-pressure air, which expands rapidly, thus making the hydrogen gas have a better penetration depth and mixing effect.

It can be seen according to Fig. 16 that the hydrogen mixing effect of the double-strut injection is significantly better than the separate injection of the upper and lower struts. The hydrogen gas at the outlet is too concentrated in the lower strut injection, and the hydrogen gas distribution width field is significantly larger in the upper strut injection than in the lower strut injection. The hydrogen distribution width is wider, and the mixing effect is better when the double-strut is injected simultaneously.

And the hydrogen molar fraction distribution curves at the outlet of single hydrogen nozzle, multiple hydrogen nozzle, and strut injection are shown in Fig. 17. The mixing effect of strut injection is much

greater than that of wall injection, and the problem of hydrogen concentration at the wall is effectively solved.

6 Summary

In this paper, the inlet of the oblique detonation engine is taken as the research object. The fuel mixing and flow field structure are analyzed and discussed through the numerical simulation method and theoretical analysis. The law of the influence of the change of jet structure and parameters on the flow field and fuel mixing is obtained. The main results are summarized as follows:

(1) According to the analysis of the structure of the single hydrogen nozzle set on the upper wall, it is found that when the equivalence ratio of hydrogen to oxygen is changed, the static pressure of the hydrogen nozzle is increased, and the dynamic pressure ratio of the hydrogen nozzle to the incoming flow is increased, so that the penetration depth is more profound, the efficiency of momentum exchange is higher, and the fuel mixing is better; When the position of the single hydrogen nozzle is changed to be close to the air inlet, the hydrogen is diffused more sufficiently due to the utilization of the length of the air inlet, so that the hydrogen mixing effect is better; when the incoming flow Mach number is changed, the dynamic pressure ratio between the hydrogen nozzle and the incoming flow is large due to low incoming flow Mach number, so that the penetration depth of hydrogen is deep, and the mixing effect is better; When changing the angle of the hydrogen nozzle, if the angle is too large or too small, the hydrogen will be more likely to cling to the wall, resulting in excessive concentration of hydrogen, and will reduce the penetration depth of hydrogen, thus reducing its mixing effect.

(2) The discovery of the aerodynamic method of setting multiple hydrogen nozzles on the upper wall. Multiple jet shock waves are formed by the obstruction of air by multiple jets. Under the condition of keeping the same hydrogen mass flow rate with a single nozzle, the more nozzles are set, the more jet shock waves are generated, and the rise of pressure, density, and temperature behind the shock waves is beneficial to increasing the diffusion efficiency of hydrogen so that the fuel mixing condition at the outlet is improved

(3) The installation of the nozzle on the walls always results in a concentration of hydrogen on the walls, which plays a crucial role in the mixing of hydrogen. Therefore, in this paper, two strut injectors parallel to the incoming flow are set at the front end of the inlet. Therefore, in this paper, two strut injectors parallel to the incoming flow are set at the front end of the inlet. The staggered hydrogen jets from the strut injectors increase the momentum exchange between hydrogen and air. The hydrogen near the wall is affected by the oblique shock wave generated by the compression with the wall. The baroclinic effect generated by the great density gradient between hydrogen and air is also beneficial to enhance fuel mixing. The most important point is that the problem of hydrogen concentration on the wall is solved by setting the strut injection at the front of the inlet, and the hydrogen mixing at the outlet of the double strut injection is obviously better than that of other examples.

Declarations

Availability of data and materials

The datasets used or analyzed during the current study are available from the corresponding author on reasonable request.

Competing interests

The authors declare that they have no known competing financial interests or personal relationships that could have appeared to influence the work reported in this paper.

Authors' contributions

Xiang Gaoxiang: Conceptualization, Methodology, Numerical simulations, Writing- Reviewing and Editing. Li Danyang: Translating, Literature research. Jie Xuzhen: Literature research, Numerical simulations, Writing- Original draft preparation. Tu Qirong: Translating and Dr Zhang Yichen: proposed some suggestions on this paper. Jin Ke: Funding.

Funding and Acknowledgements

This work was supported by the National Numerical Wind tunnel project (NNW2020ZT3-A23), the Guangdong Basic and Applied Basic research Foundation (2022A1515011565), Foundation of State Key Laboratory of High Temperature Gas Dynamics (2021KF10), and the China Postdoctoral Science Foundation funded project (2021M692633).

References

1. Cheng J, Zhang B, Ng HD, Liu H, Wang FX (2021) Effects of inert gas jet on the transition from deflagration to detonation in a stoichiometric methane-oxygen Fuel. 285:119237
2. Jiang Z, Zhang Z, Liu Y, Wang C, Luo C (2021) Criteria for hypersonic airbreathing propulsion and its experimental verification. Chin J Aeronaut 34:94–104
3. Uy KCK, Shi LS, Wen CY (2020) Numerical analysis of the vibration chemistry coupling effect on one-dimensional detonation stability. Aerosp Sci Technol 107:106327
4. Saxena S, Kahandawala MSP, Sidhu SS (2011) A shock tube study of ignition delay in the combustion of ethylene. Combust Flame 6:1019–1031
5. Bhatrai S, Tang H (2017) Formation of near-Chapman-Jouguet oblique detonation wave over a dual-angle ramp. Aerosp Sci Technol 63:1–8
6. McGarry JP, Ahmed KA (2017) Flame-turbulence interaction of laminar premixed deflagrated flames[J]. Combust Flame 176:439–450. DOI: 10.1016/j.combustflame.2016.11.002

7. Frolov SM, Dubrovskii AV Ivanov VS. Three-dimensional. Numerical simulation of the operation of a rotating-detonation. Chamber with separate supply of fuel and oxidizer[J]. Combustion, Explosion and Shock Waves, 2013, 32(2):56–65
8. Rosato DA, Thornton M, Sosa J et al (2021) Stabilized detonation for hypersonic propulsion. Proc Natl Acad Sci USA 118:e2102244118
9. Rudy W, Dziubanii K, Zbikowski M et al (2016) Experimental determination of critical conditions for hydrogen-air detonation propagation in partially confined geometry. International Journal of Hydrogen Energy, 1–8
10. Maeda S, Inada R, Kasahara J, et al et al (2011) The stabilized oblique detonation wave and unsteady wave structure around hyper-velocity spherical projectile[R]. AIAA-2011-505,
11. Yu Lujun F, Baochun G, Mingyue, Dong Gang (2009) Study on the outflow field of exit detonation[J]. J Mech 41(1):28–34
12. Martínez-Ruiz D, Huete C, Sánchez AL et al (2020) Theory of weakly exothermic oblique detonations. AIAA J 58:236–242
13. Wang K, Teng H, Yang P et al (2020) Numerical investigation of flow structures resulting from the interaction between an oblique detonation wave and an upper expansion corner[J]. Journal of Fluid Mechanics, 903
14. Baurle R, Mathur T, Gruber M et al (2013) A numerical and experimental investigation of a scramjet combustor for hypersonic missile applications[C]. Proceedings of the 34th AIAA/ASME//SAE/ASEE Joint Propulsion Conference and Exhibit, Joint Propulsion Conferences, Cleveland, OH, USA: AIAA,
15. Abdelsalam T, Tiwari S, Mohieldin T (2013) Effects of ramp swept angle in supersonic mixing [C].
16. Fuller RP, Nejad AS, Schetz JA et al (1998) Comparison of Physical and Aerodynamic Ramps as Fuel Injectors in Supersonic Flow [J]. J Propul Power 14(2):135–145
17. Fuller R, Wu PK, Nejad A et al (1996) Fuel-vortex interactions for enhanced mixing in supersonic flow [C].
18. Stallings R, Wilcox F (1987) Experimental cavity pressure distributions at supersonic speeds [J]. Nasa Tp.
19. Fusina G, Sislian JP, Parent B (2005) Formation and Stability of Near Chapman-Jouguet Standing Oblique Detonation Waves[J]. Aiaa J 43(7):1591–1604
20. Vlasenko VV, Sabel'Nikov VA (1995) Numerical simulation of inviscid flows with hydrogen combustion behind shock waves and in detonation waves [J]. Combust Explosion Shock Waves 31(3):376–389
21. Cambier JL, Adelman H, Menees GP (1990) Numerical simulations of an oblique detonation wave engine [J]. J Propuls Power 6(3):L24801
22. Sislian JP, Dudebout R, Schumacher J et al (2000) Incomplete Mixing and Off-Design Effects on Shock-Induced Combustion Ramjet Performance [J]. J Propuls Power 16(1):41–48

23. Iwata K, Nakaya S, Tsue M (2016) Numerical Investigation of the Effects of Nonuniform Premixing on Shock-Induced Combustion [J]. *Aiaa J* 54(5):1–11
24. Iwata K, Nakaya S, Tsue M (2016) Wedge-stabilized oblique detonation in an inhomogeneous hydrogen-air mixture [J]. *Proceedings of the Combustion Institute*. : S1881661741
25. Fang Yishen (2019) Study on the mechanism of oblique detonation formation under the action of complex wave system[D]. University of Chinese Academy of Sciences
26. Sislian JP, Martens RP, Schwartzentruber TE et al (2015) Numerical Simulation of a Real Shramjet Flowfield [J]. *J Propuls Power* 22(5):1039–1048
27. Zhang Zijian (2020) Theory, technology, and experimental validation of oblique detonation propulsion [D]. University of Chinese Academy of Sciences, Beijing
28. Zhang Z, Liu Y, Jiang Z(2019) Numerical Investigations of a Mach 9 Oblique Detonation Wave Engine with Fuel Pre-injection[C].
29. Oran ES (2013) Numerical simulations of hydrogen detonations with detailed chemical kinetics. *Proceedings of the Combustion Institute*, 34: 2009–2016
30. Sharpe GJ, Quirk JJ (2007) Nonlinear cellular dynamics of the idealized detonation model: regular cells. *Combust Theor Model* 12(1):1–21
31. Honghui T, Chun W, Wei Z (2011) Numerical study of complex structures on oblique detonation wavefront[J]. *J Mech* 43(4):641–645
32. Ng HD, Botros BB, Chao J (2006) et al. Head-on collision of a detonation with a planar shock wave. *Shock Waves* 15:341N352

Figures

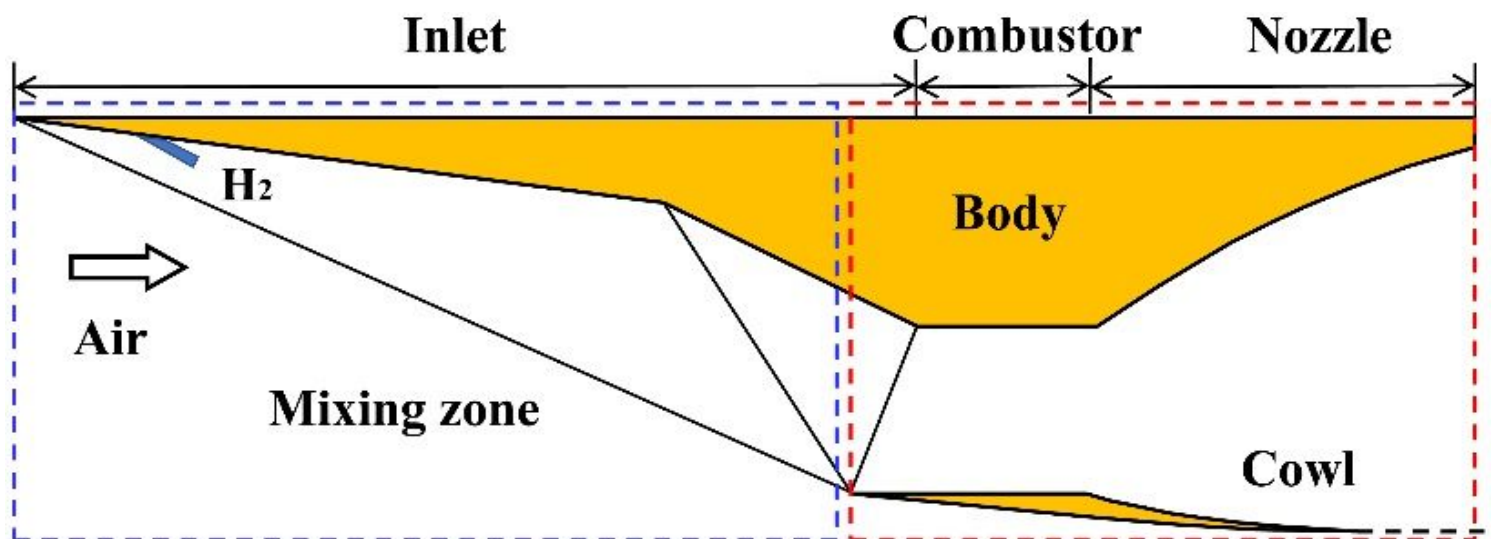


Figure 1

Physical model

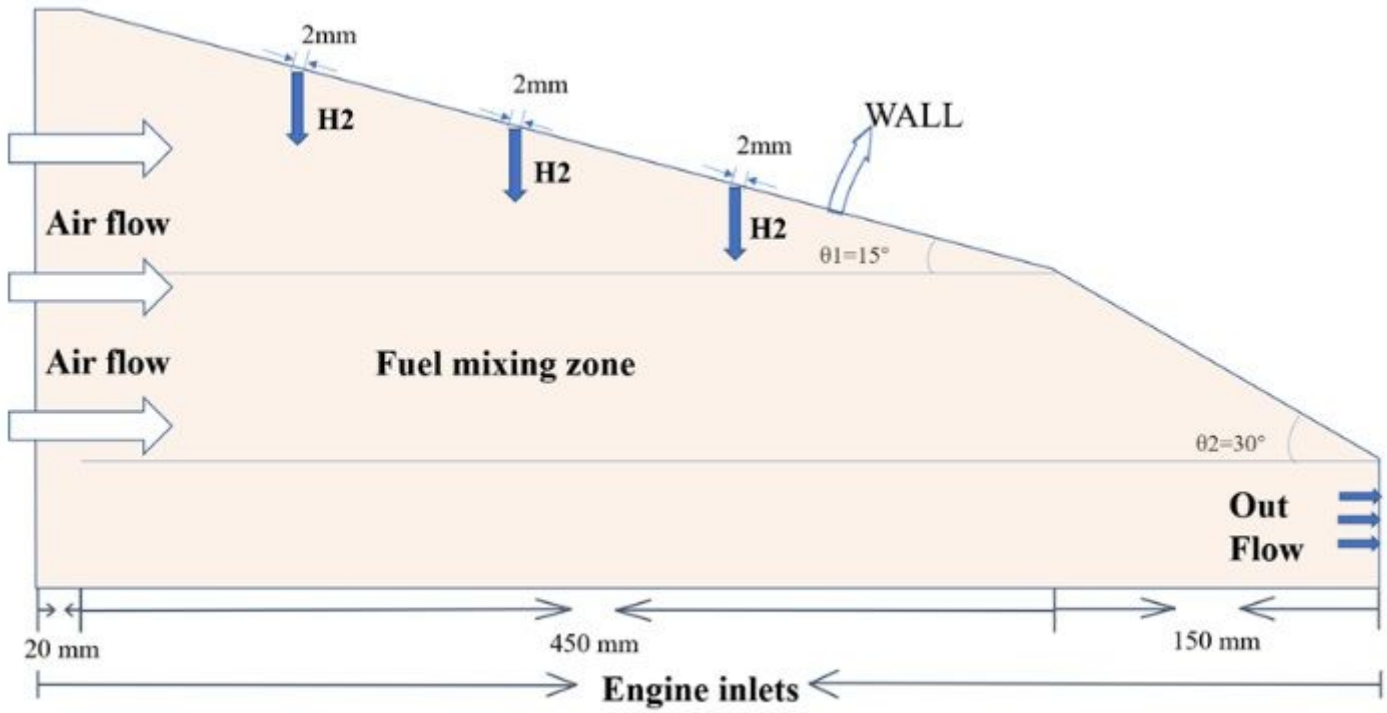


Figure 2

Schematic diagram of the computational domain

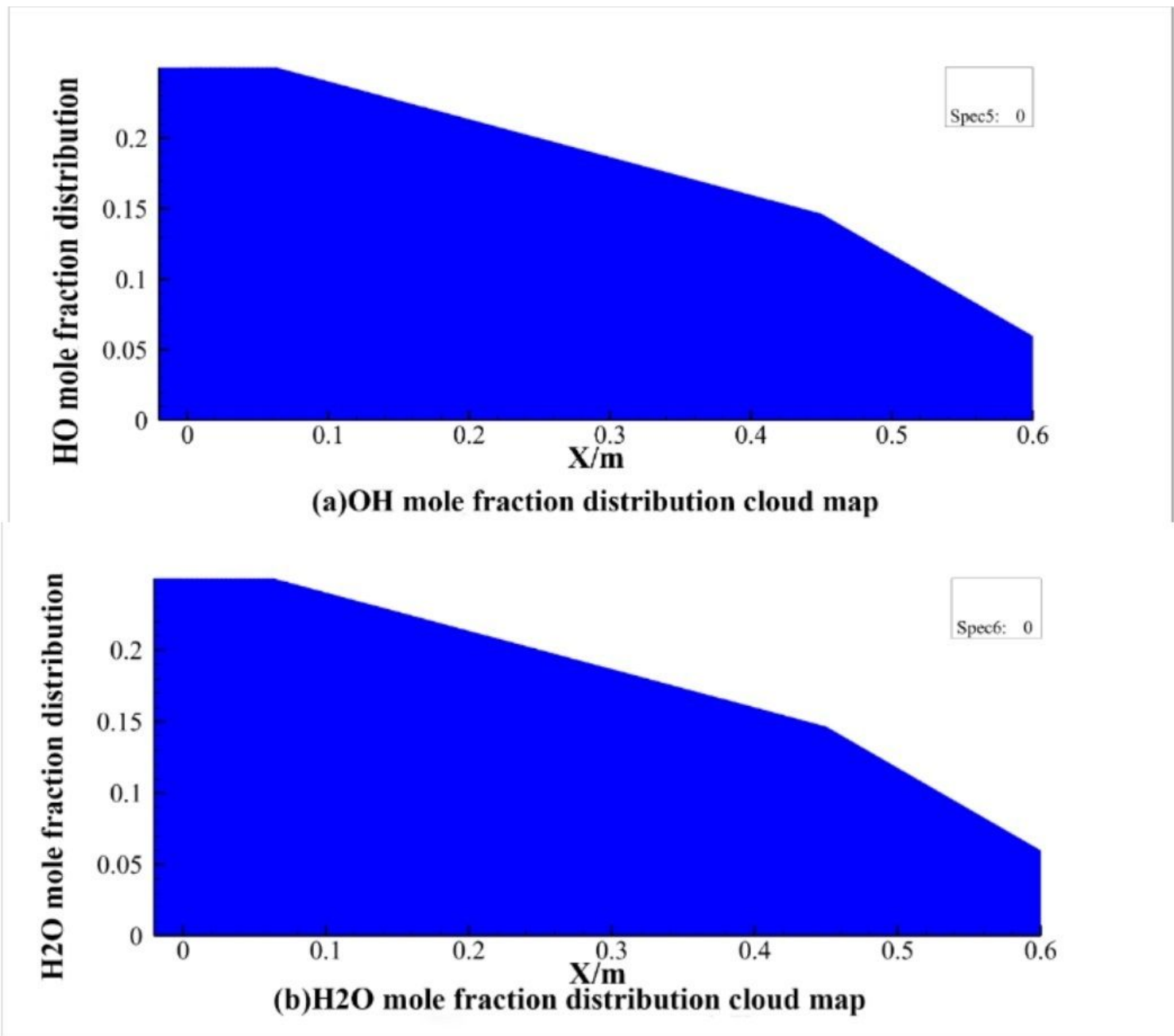


Figure 3

Flammability assessment chart

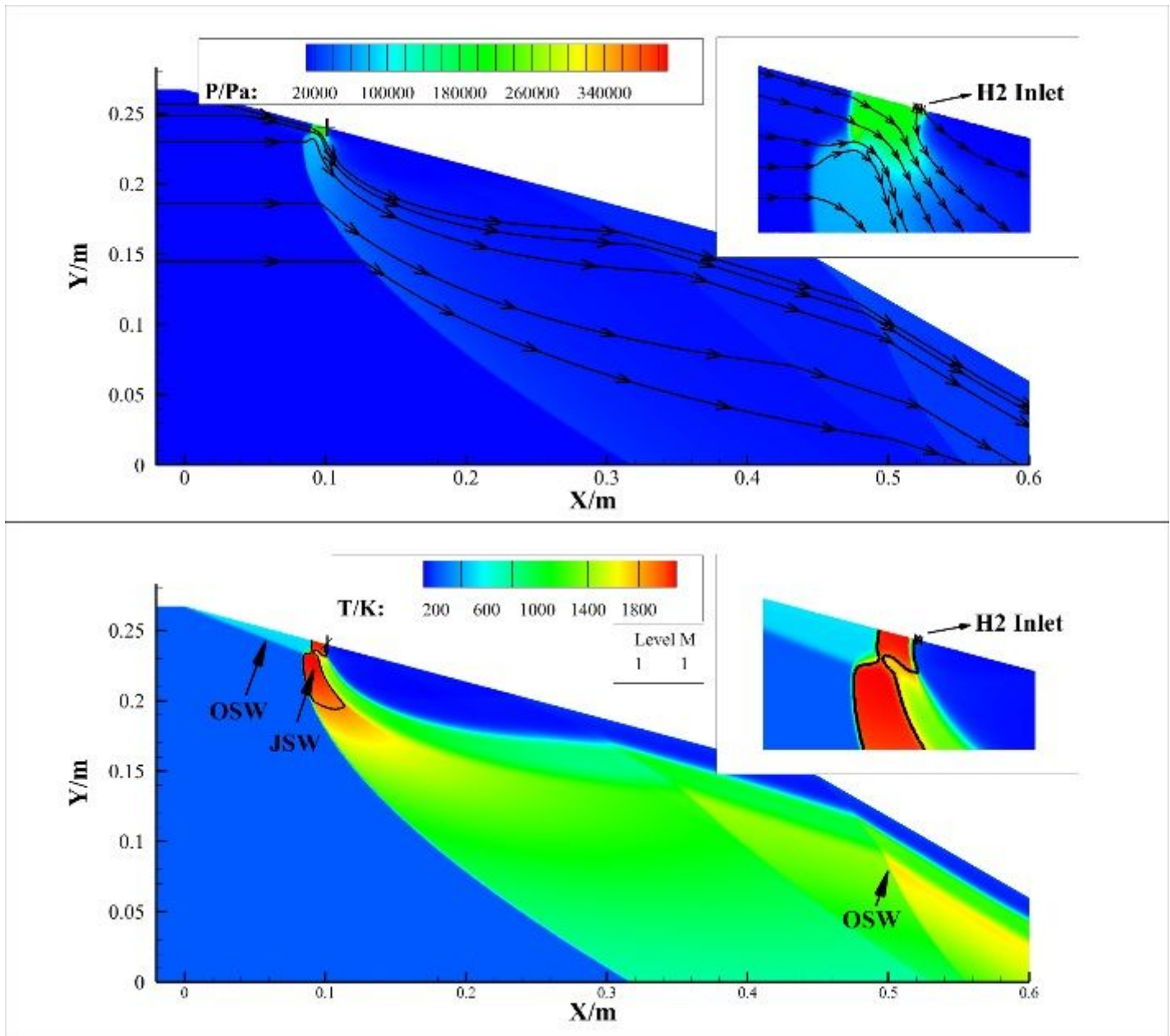


Figure 4

Flow field structure of single hydrogen nozzle

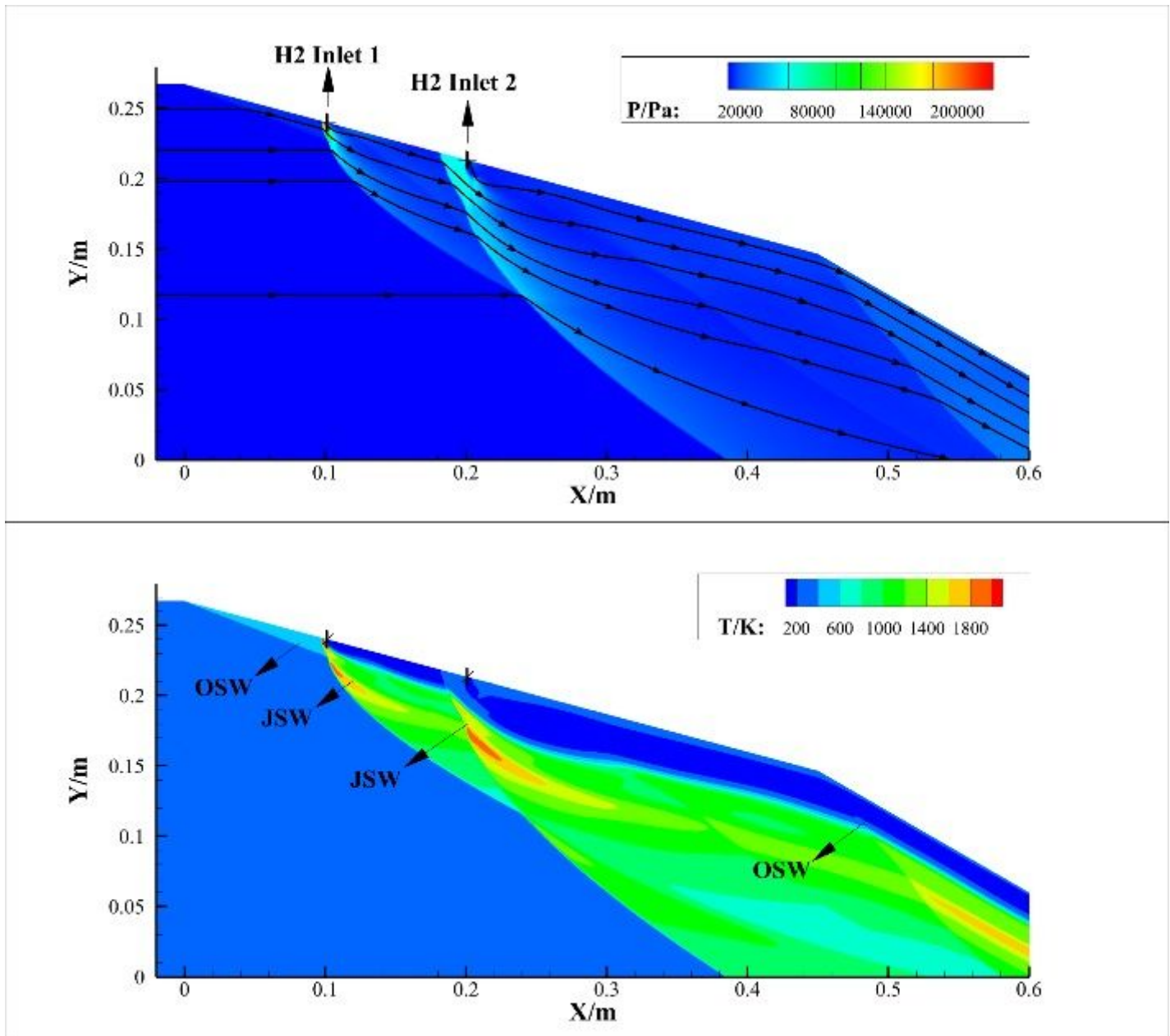


Figure 5

Flow field structure of double hydrogen nozzle

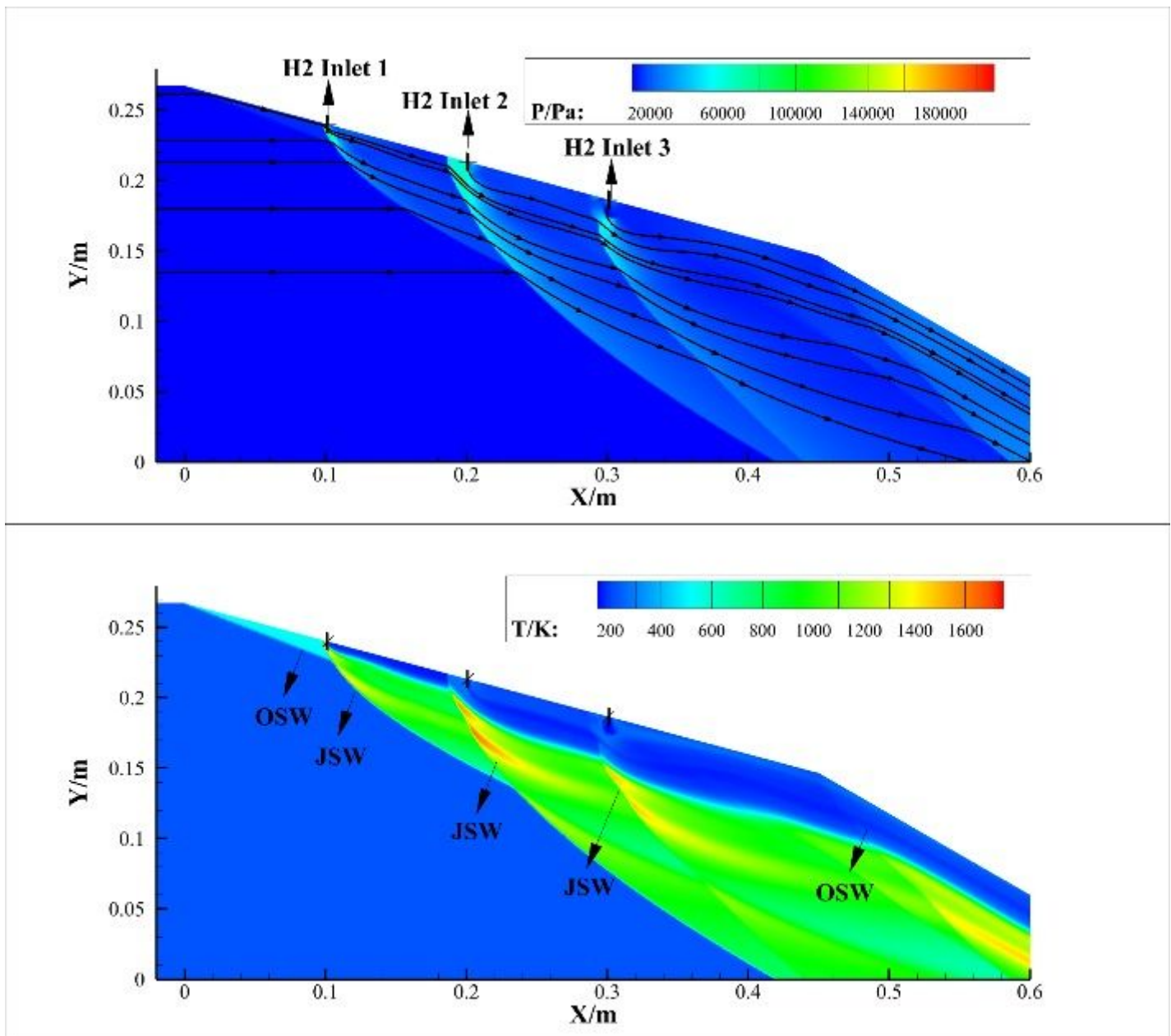


Figure 6

Flow field structure of triple hydrogen nozzle

Figure 7

Effect of hydrogen to oxygen equivalent ratio

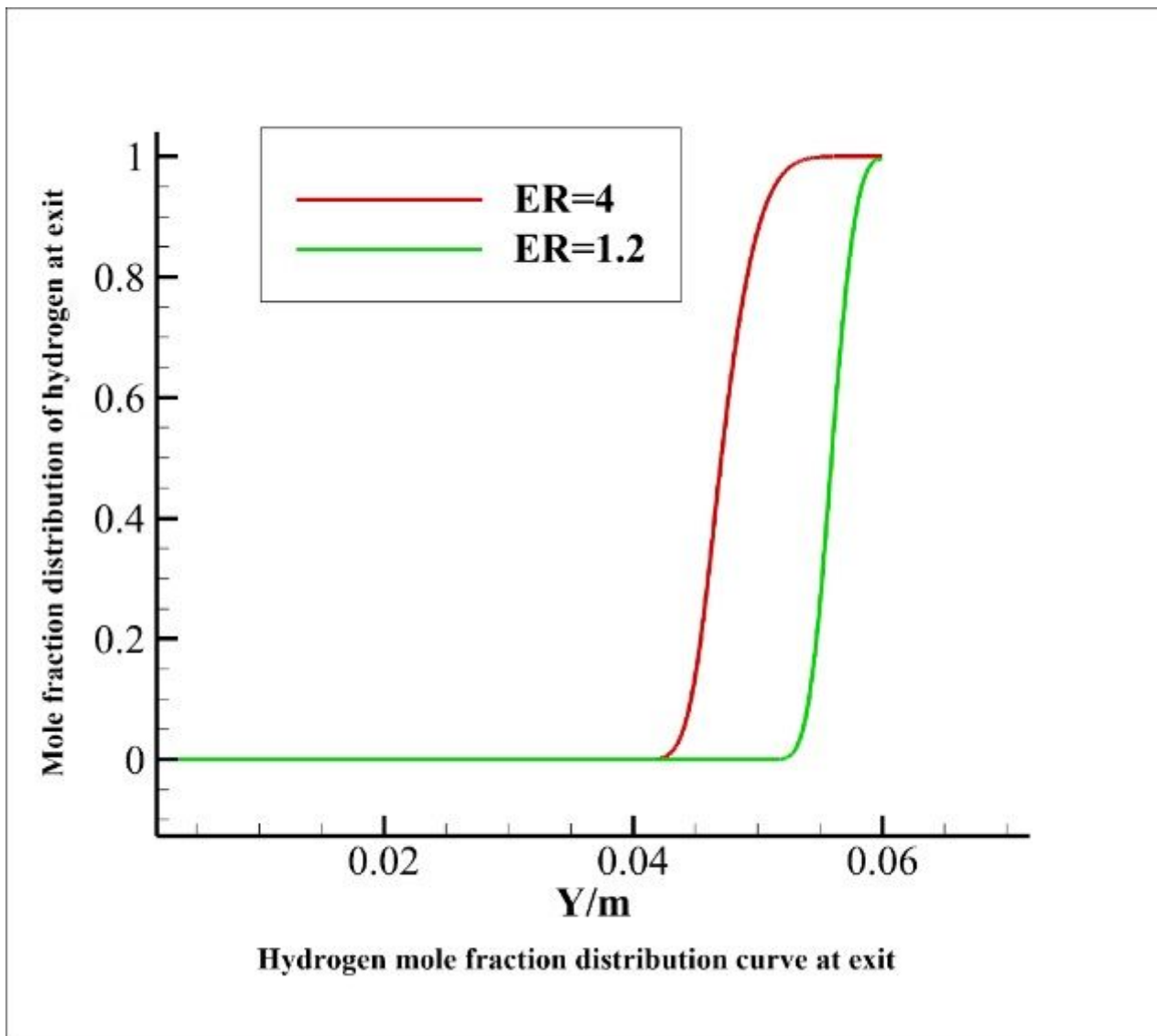


Figure 8

Molar fraction distribution curve of hydrogen with different hydrogen to oxygen equivalent ratios at the outlet

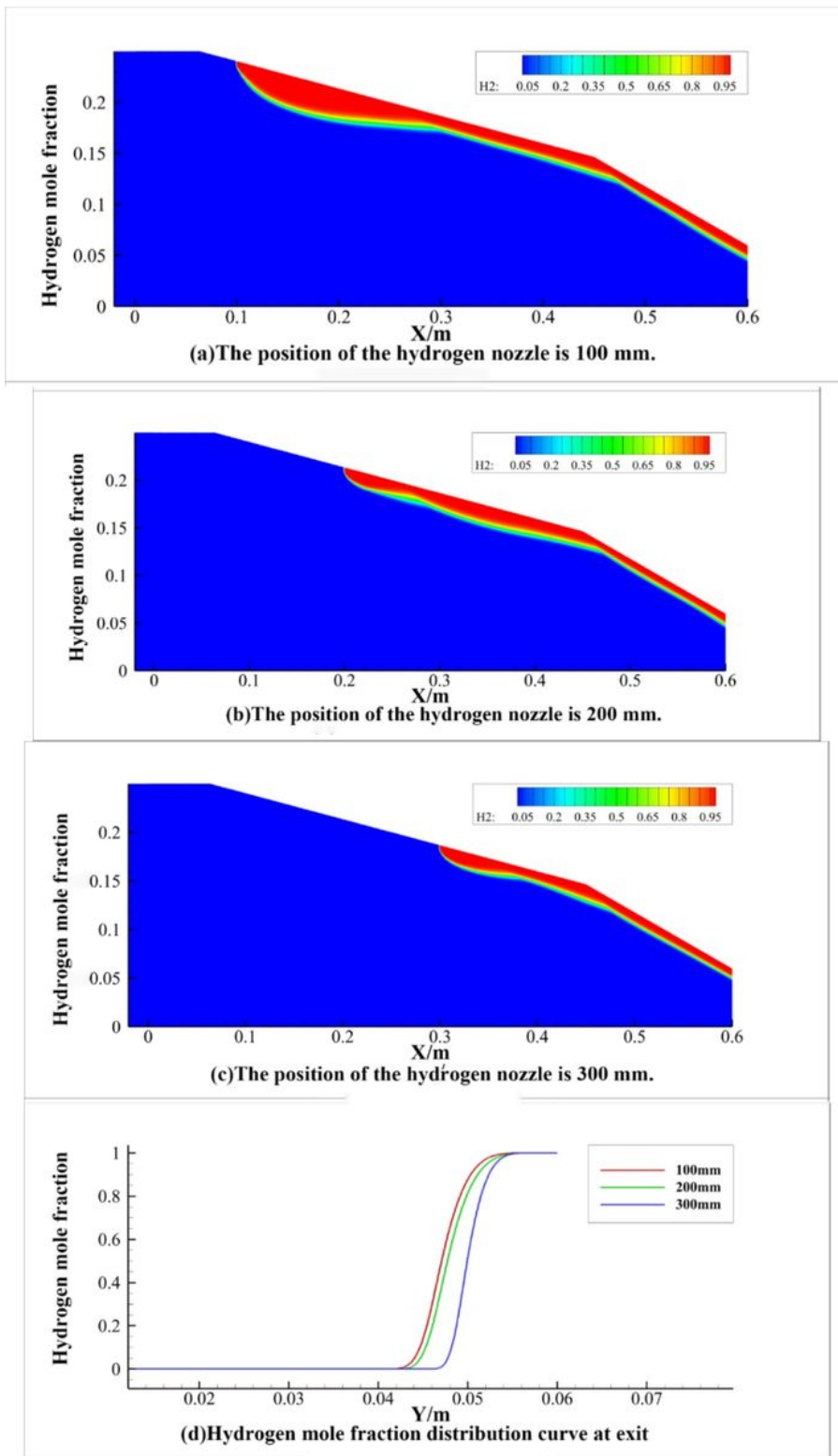


Figure 9

Effect of hydrogen vent location

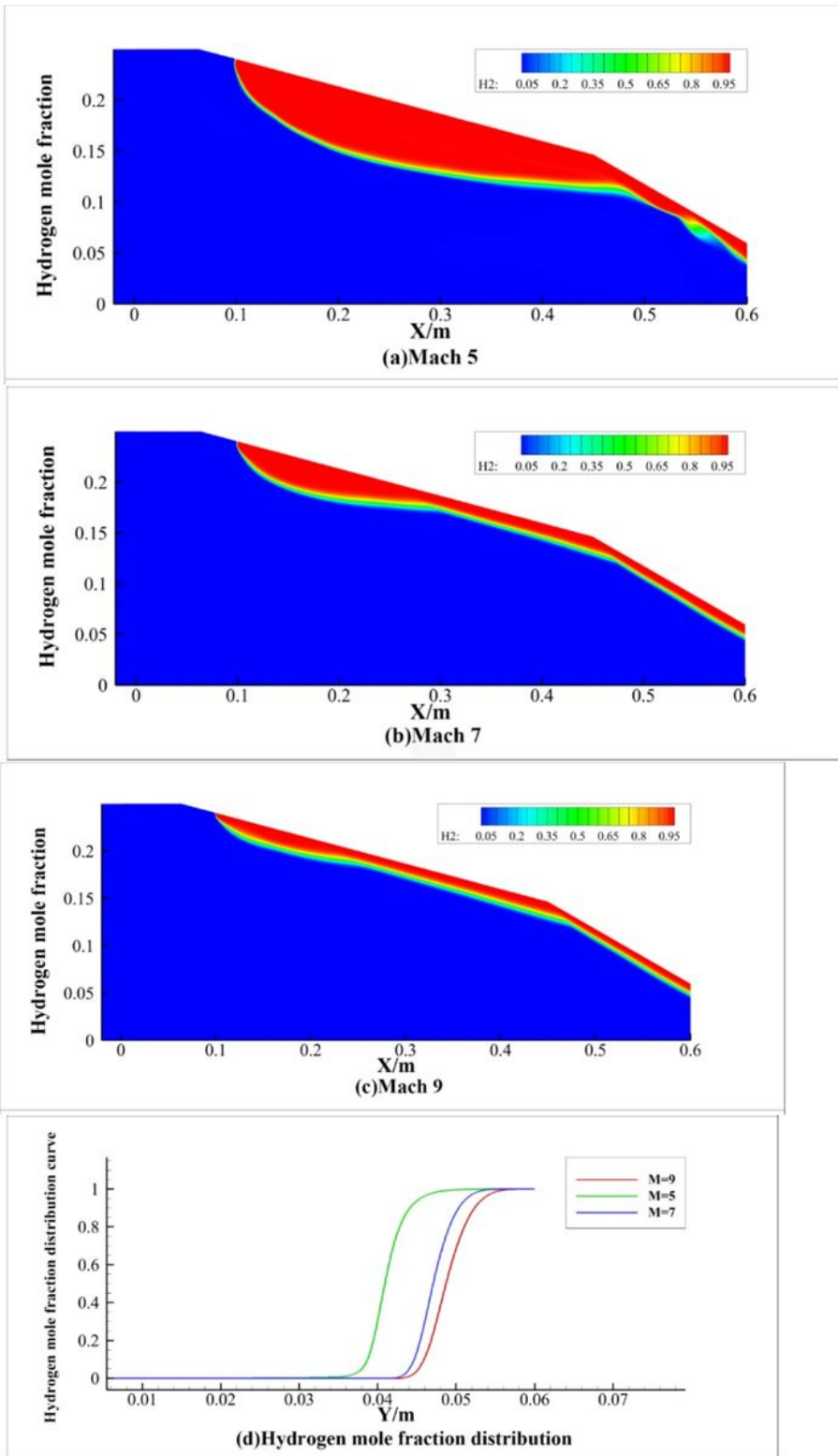


Figure 10

Effect of incoming Mach number

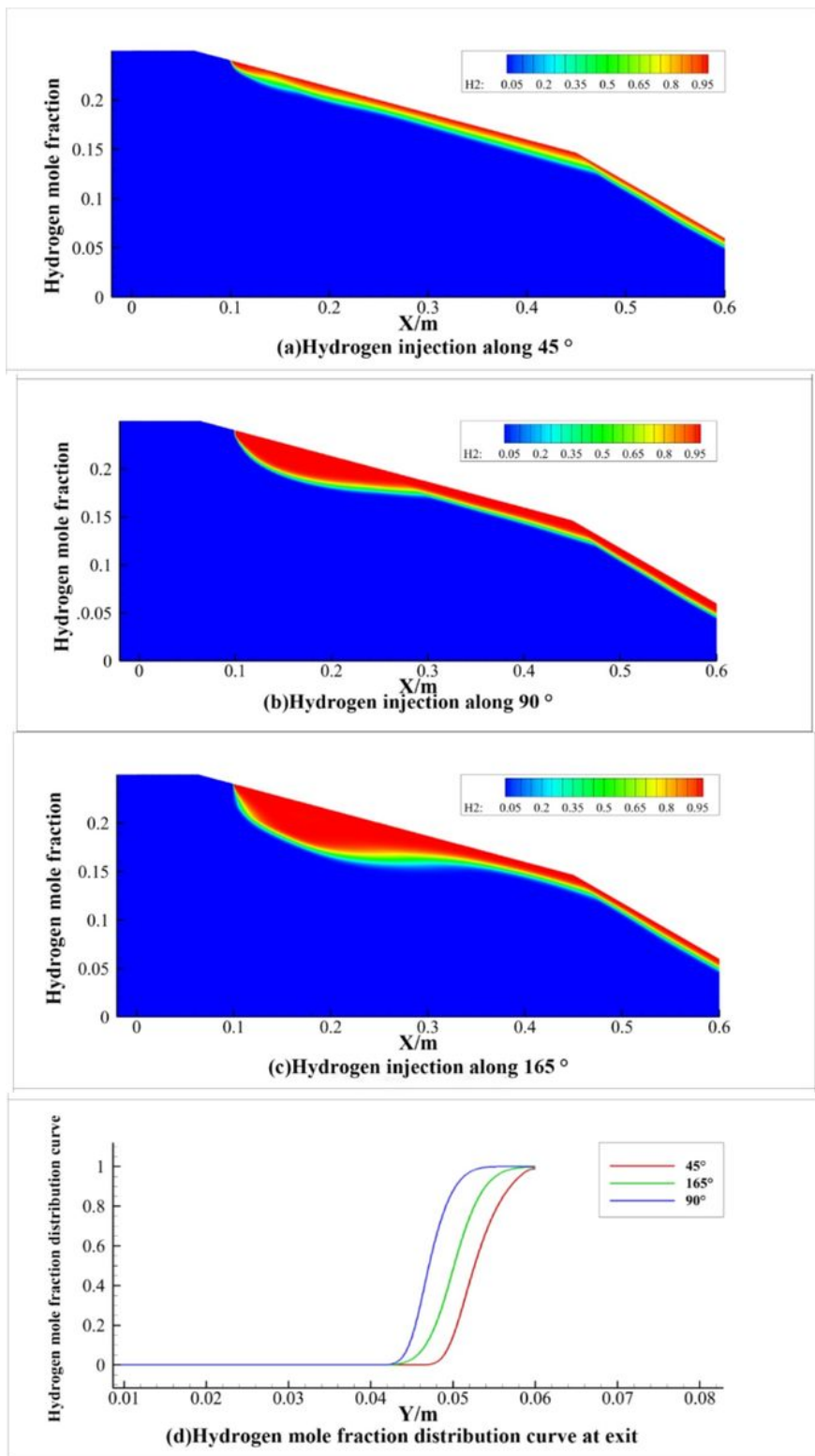


Figure 11

Effect of hydrogen injection angle

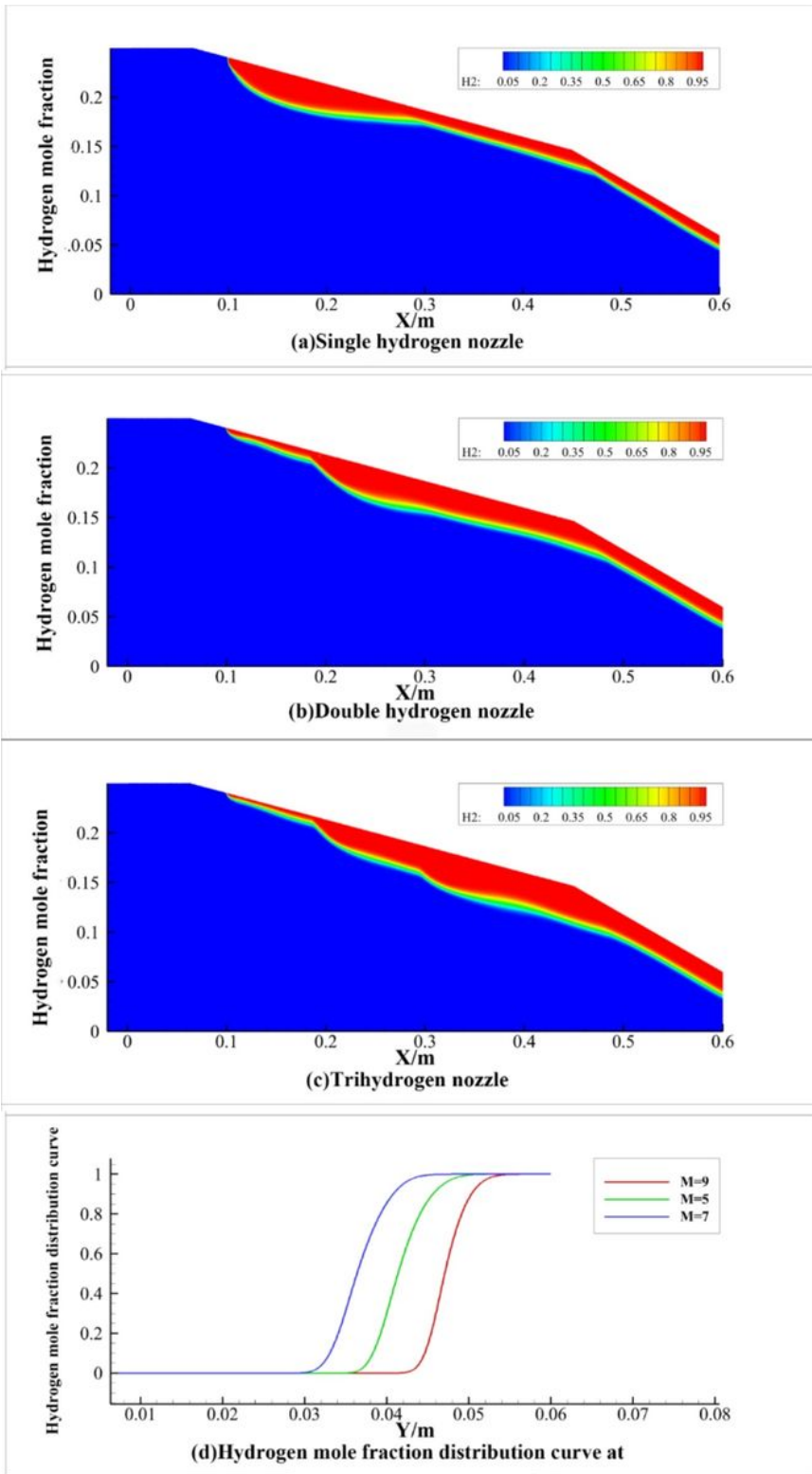


Figure 12

12 Effect of the number of hydrogen vents

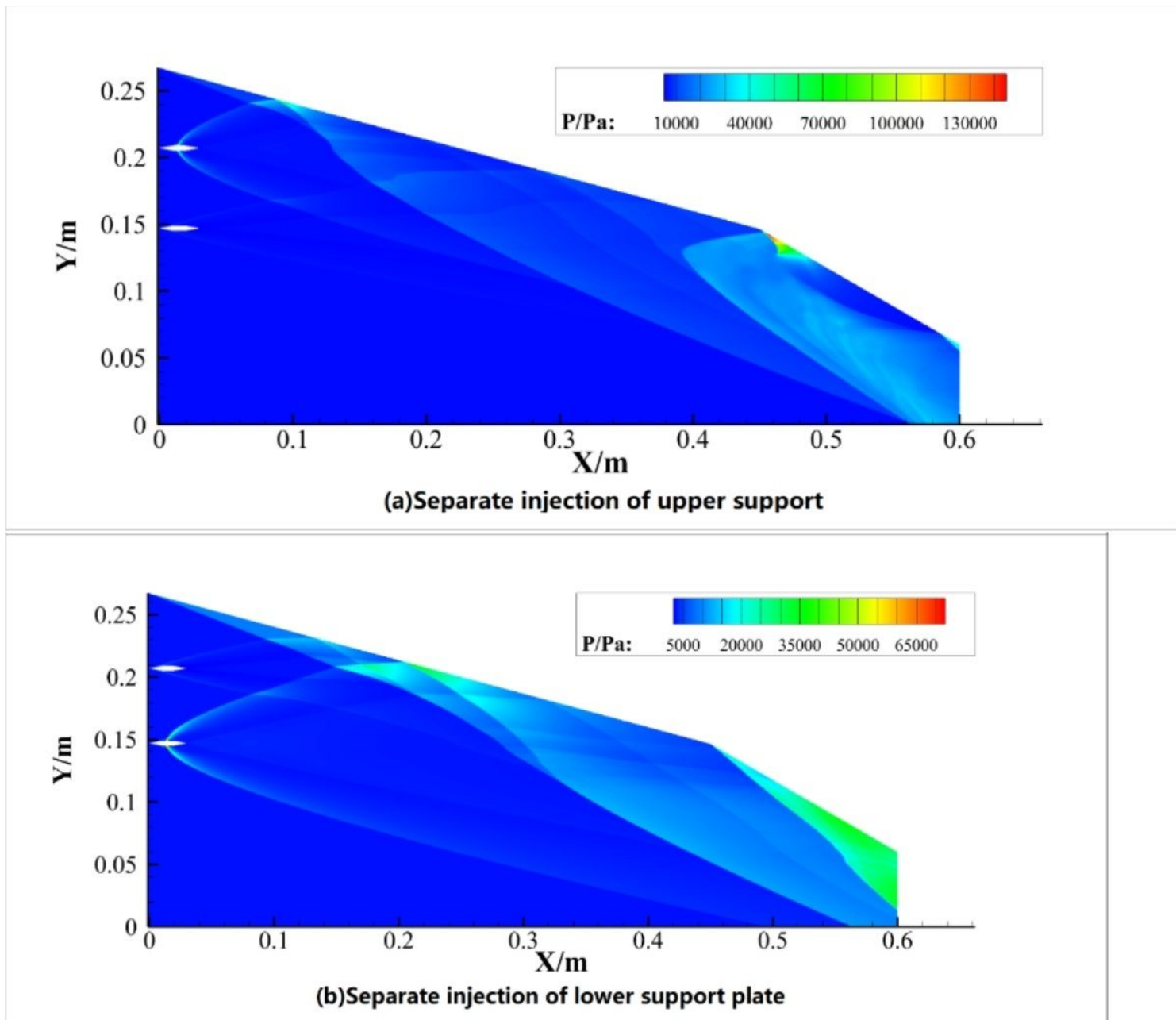


Figure 13

Flow field structure of the upper and lower branch plate with separate injection

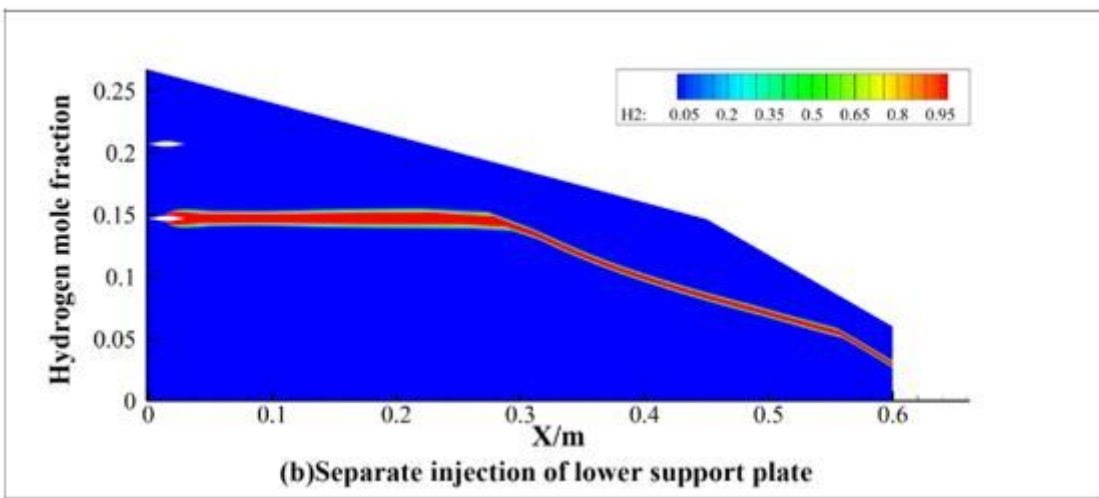
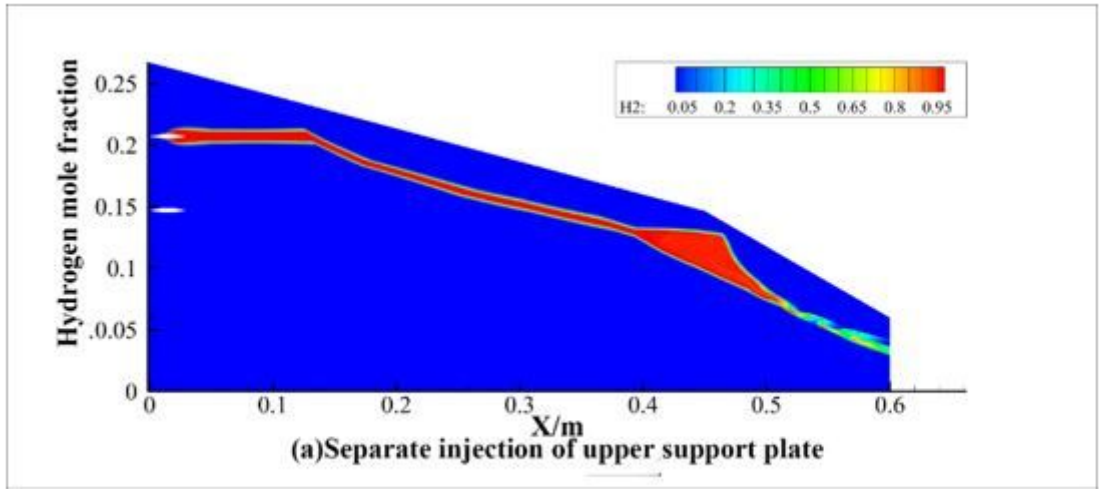


Figure 14

Distribution of hydrogen gas injected separately from the upper and lower branch plates

Figure 15

Flow field structure and hydrogen distribution of double-branch plate injection

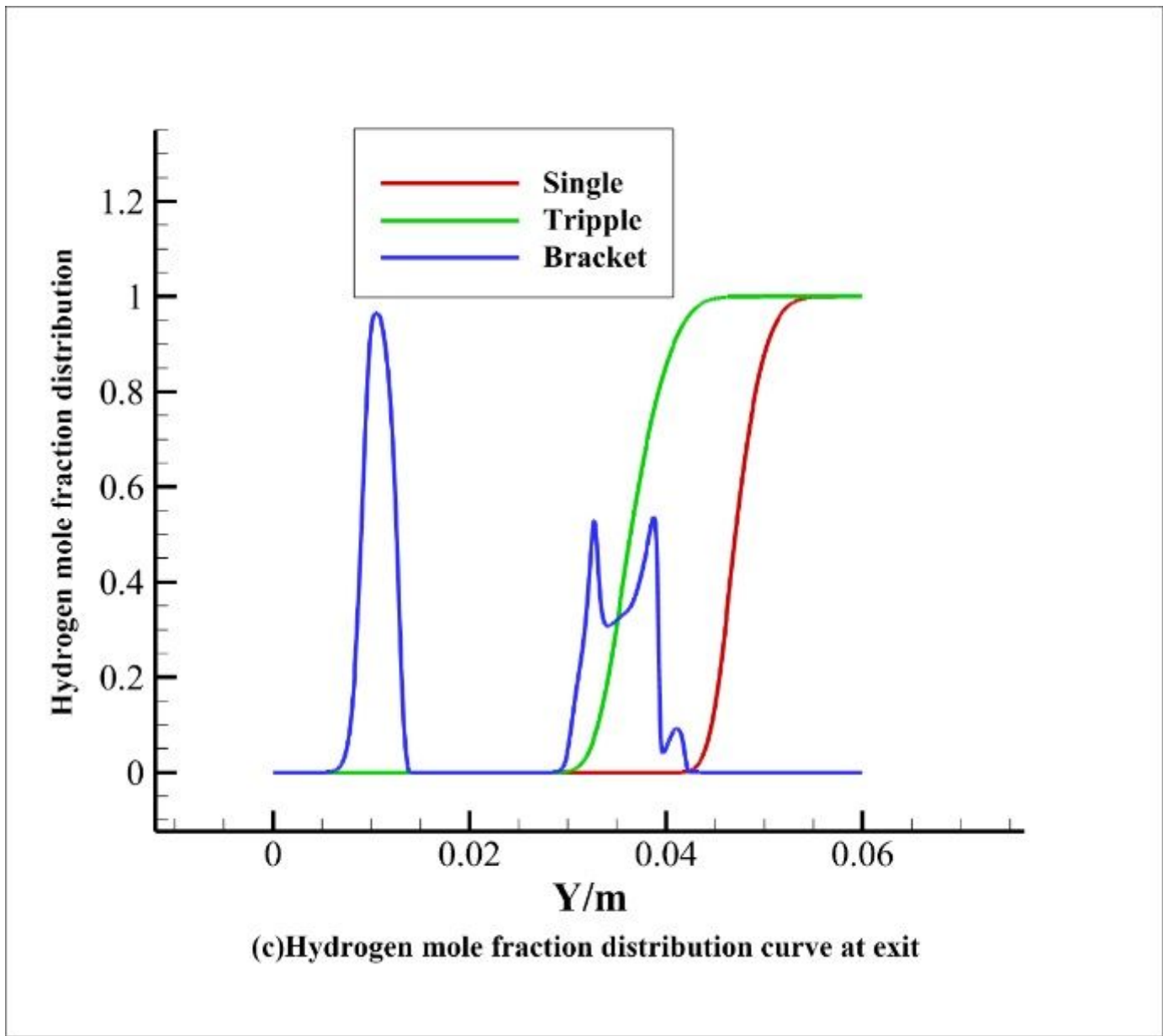


Figure 16

Hydrogen molar fraction distribution curve at the outlet during branch plate injection

Figure 17

Hydrogen molar fraction distribution curve at the outlet of single hydrogen orifice, multiple hydrogen orifices and branch plate injection